23RD INTERNATIONAL SYMPOSIUM ON BALLISTICS
TARRAGONA, SPAIN 16-20 APRIL 2007

ANALYTICAL SOLUTIONS FOR THE LINEAR AND NONLINEAR YAWING MOTION IN DENSE MEDIA

Paul Weinacht[1] and Gene R. Cooper[1]

[1]*US Army Research Laboratory, Aberdeen Proving Ground, MD 21005-5066*

Analytical solutions for the linear and nonlinear yaw growth of a projectile impacting and traversing dense media are presented. From the linear solution, it is shown that Roecker's linear exponential yaw growth model can be obtained from the general solution for arbitrary impact yaw and yawing rates after a sufficient depth of penetration. However, using the general solution, it is shown that Roecker's yaw growth model does not adequately represent the yaw growth during the initial phase of the penetration event. Analytical solutions for the nonlinear yaw growth are then presented. For the particular form of the overturning moment considered here, the nonlinear yaw growth is characterized by oscillating motion at yaw angles less than 180 degrees or by an end-over-end tumbling motion, depending on the striking yaw and yawing rate. A limiting case motion between the two regimes is also possible but physically unlikely. However, the limiting case motion represents an approximation of the nonlinear exponential yaw growth over a significant portion of the penetration event for the general case, provided the striking yaw and yawing rate are small. This validates its use as a representation for the nonlinear yaw growth in prior work.

INTRODUCTION

The yawing motion of projectiles in dense media is significantly different than free-flight yawing motion in air. In particular, for spin (gyroscopically) stabilized projectiles, the increase in media density between air and a more dense medium, such as water, soil, or tissue simulants, is sufficient to reduce the gyroscopic stability so that the projectile is stable in air but unstable in dense media. This instability produces a rapid increase in yaw to very large angles as the projectile traverses the dense media.

The yawing behavior of projectiles in dense media has been investigated previously from both theoretical and experimental points of view[1,2]. One important result, obtained by Roecker [1], forms the current theoretical basis for characterizing important aspects of projectile yawing behavior in dense media. Using a simple linear equation of motion, Roecker [1] has obtained an analytical solution for the yawing motion of an unstable bullet in dense media. Roecker also obtained a numerical solution of the large angle nonlinear form of the governing equation. Roecker used his theoretical results as a basis for correlating experimental data, and the results (shown in Fig. 1) seem to show excellent agreement with the derived form. More recently, Flis [2] obtained an analytical solution to the nonlinear form of the governing equation that was solved numerically by Roecker. This solution provides a relatively simple analytical form for Roecker's numerical results and extends Roecker's analytical solution of the linear governing equation to larger penetration depths and high yaw angles.

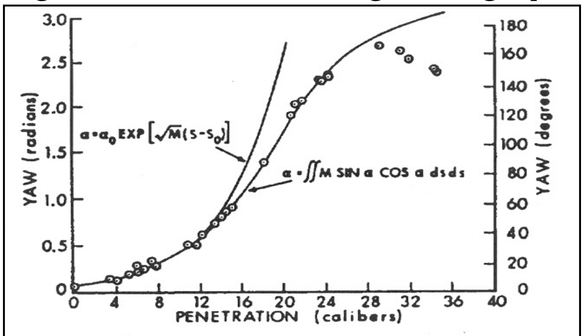

Fig. 1. Correlation of experimental yaw data using Roecker's theoretical results, from Ref [1].

Unfortunately, the mathematical basis for Roecker's analytical solution to the linear governing equation (and subsequent numerical solution) is suspect because the initial conditions were not properly applied when the solution was developed. (Similar observations have been made independently by Flis [2].) The result is that Roecker's solution does not properly characterize the yawing motion of projectile in dense media, particularly during the early phase of the penetration event. It is possible, however, to obtain general analytical solutions to both the linear and nonlinear governing equations that are mathematically sound and are valid for a more general set of initial conditions. The yaw growth behavior from the solutions of the linear governing equations is shown here to asymptotically approach Roecker's linear exponential yaw growth model for increasing penetration depth. The solutions also reconcile the initial conditions corresponding to Roecker's linear exponential yaw growth model with the local yaw angles and angular rates exhibited by an unstable projectile during the penetration event. Analytical solutions to the nonlinear governing equation are also obtained which complement the numerical solutions obtained by Flis [2]. The results expose important insights into the physical behavior of yawing projectiles in dense media and set the foundation for correctly using the functional forms proposed by Roecker and Flis.

THE NONLINEAR AND LINEAR GOVERNING EQUATIONS

The derivation of the governing equation used as a basis for developing the analytical solution is shown below. From Newton's Second Law, the rate of change of angular momentum of the projectile with respect to time is equal to the applied moment.

$$I_t \frac{d^2\alpha}{dt^2} = \frac{1}{2}\rho V^2 S_{ref} D_{ref} C_{m_\alpha} \sin\alpha \cos\alpha \tag{1}$$

Here, α is the yaw angle, I_t is the transverse moment of inertia of the projectile, ρ is the media density, V is the projectile velocity, D_{ref} is the reference diameter, S_{ref} is the reference area, and C_{m_α} is the pitching moment coefficient. The nonlinear form of the applied fluid dynamic moment is based on slender body theory as shown previously by Roecker.

The independent variable can be transformed from space to time, and the relative effect of the deceleration is assumed small. The remaining coefficients shown in Eq. 2 can be represented by a single constant, assuming invariance with velocity and yaw angle.

$$\frac{d^2\alpha}{ds^2} = M \sin\alpha \cos\alpha \quad \text{where} \quad M = \frac{1}{2I_t}\rho S_{ref} D_{ref} C_{m_\alpha} \tag{2}$$

M can be positive or negative depending on whether the projectile is statically stable or unstable. The focus of the current effort is on characterizing the yawing performance of projectiles that are statically unstable. For the remainder of the report, it is assumed that M is positive. A linearized form of the governing equation, valid for small angles, can be obtained from the nonlinear equation approximating $\sin\alpha\cos\alpha \cong \alpha$. Both the linear and nonlinear second-order differential equations are subject to the following general initial conditions at s_0.

$$\alpha(s_0) = \alpha_0 \qquad \frac{d\alpha}{ds}(s_0) = \alpha_0' \tag{3}$$

SOLUTION OF THE LINEAR GOVERNING EQUATION

The solution to the governing linear ordinary differential equation after the application of the initial conditions is shown in Eq. 4.

$$\alpha(s) = \frac{1}{2}(\alpha_0 + \frac{\alpha_0'}{\sqrt{M}})\exp(\sqrt{M}(s-s_0)) + \frac{1}{2}(\alpha_0 - \frac{\alpha_0'}{\sqrt{M}})\exp(-\sqrt{M}(s-s_0)) \tag{4}$$

However, Roecker obtained his solution by arguing that the contribution of the damped exponential term of the general solution decreases rapidly with distance and can be ignored. By ignoring this term and then applying the initial condition $\alpha(s_0) = \alpha_0$, he obtains the following solution.

$$\alpha(s) = \alpha_0 \exp(\sqrt{M}(s-s_0)) \tag{5}$$

The approach of neglecting portions of the general solution and then applying initial conditions is not mathematically well founded. Even if the initial angular rate effect can be ignored, as the penetration depth increases, Eq. 4 yields only half of the initial yaw angle at the point where the initial conditions are applied and not the initial yaw angle as proposed by Roecker in Eq. 5.

A more rigorous derivation of Roecker's form can be obtained by examining the solution obtained in Eq. 4. Such a solution should provide more physical insight into why Roecker's correlation is valid. At a large enough penetration depth s_p, the yawing rate (determined from the derivative of Eq. 4) can be related to the yaw angle in a very simple manner because the damped exponential term in both equations becomes small.

$$\alpha'(s_p) = \alpha(s_p)\sqrt{M} \tag{6}$$

Since the initial conditions can be applied at any point along the penetration event, Eq. 4 can be reduced to a very simple form that resembles Roecker's solution.

$$\alpha(s) = \alpha(s_p)\exp(\sqrt{M}(s - s_p)) \tag{7}$$

The importance of this result is that it shows that when the depth of penetration is large enough, the subsequent yaw growth beyond a given penetration depth s_p depends only on the instantaneous yaw angle α_p. Eq. 7 appears to be consistent with the form proposed by Roecker. Significantly, α_p in Eq. 7 is not the striking yaw at the beginning of penetration event. However, Eq. 4 shows there is a transitional region where the yaw versus penetration depth should not be expected to vary as the simple exponential form proposed by Roecker (Eq. 7) and the yaw growth depends on the striking yaw and yawing rate. It is only after a sufficient depth of penetration that the instantaneous yaw angle and yawing rate are proportional (Eq. 6) and the yaw growth appears to be proportional only to the instantaneous yaw angle. In this regime, the yaw growth should correlate with the exponential form proposed by Roecker.

SOLUTION OF THE NONLINEAR GOVERNING EQUATION

The small angle assumption required to derive the linear governing equation and analytical solution can be removed by directly solving the nonlinear governing equation. This allows solutions to be obtained for higher yaw angles than for the linear solution. The solution is complicated by the fact that the governing equation is now nonlinear, but the form of the governing equations is similar to other equations (nonlinear pendulum equation, for instance) and solution methods exist for this type of nonlinear equation. Depending on the initial conditions, the solution can take different forms. Flis previously obtained analytical solutions for one particular set of initial conditions and numerical results for a variety of other initial conditions. The current analysis presents the analytical solutions for the complete range of initial conditions.

The analysis performed by Flis shows that the first integration of the second-order nonlinear governing differential equation produces Eq. 8.

$$\frac{1}{M}\left(\frac{d\alpha}{ds}\right)^2 = \sin^2\alpha - \kappa \qquad \text{where} \qquad \kappa = \sin^2\alpha_0 - \frac{1}{M}\left(\frac{d\alpha}{ds}\right)_0^2 \tag{8}$$

Depending on the value of κ, the solution of Eq. 8 takes different forms. Three cases have been identified. Note that κ can never be greater than one because $\sin\alpha_0$ will never be greater than one and the second term will always be negative for positive values of the yaw growth parameter M.

Case 1 (Oscillating Solutions): $(0 < \kappa < 1)$. The solution for the first case has the following form where $\mathrm{dn}(u\,|\,m)$ is one of the Jacobi elliptic functions. This function is also written as $\mathrm{dn}(u, \sqrt{m})$ in traditional texts.

$$\alpha = \sin^{-1}\left[\mathrm{dn}\left(\sqrt{M}(s - s_0 + \hat{s})\,|\,1-\kappa\right)\right] \tag{9}$$

This solution will provide the solution for yaw angles up to $\pi/2$ (assuming the striking yaw is below $\pi/2$) or alternatively over the interval $0 \le s - s_0 + \hat{s} - n4K \le 2K$ where K is the period of the elliptic function and n is an integer so that $0 \le s - s_0 + \hat{s} - n4K \le 4K$. To obtain the solution as the yaw angles continue to increase above $\pi/2$, a different branch of the solution must be used.

$$\alpha = \pi - \sin^{-1}\left[\mathrm{dn}\left(\sqrt{M}(s - s_0 + \hat{s})\,|\,1-\kappa\right)\right] \tag{10}$$

This solution is valid over the interval $2K \le s - s_0 + \hat{s} - n4K \le 4K$. $\hat{s}$ is determined from the initial conditions (assuming the striking yaw is less than $\pi/2$) so that $\sin\alpha_0 = \mathrm{dn}\left(\sqrt{M}\;\hat{s}\;|\,1-\kappa\right)$

and

$$\alpha_0' = \frac{-1}{\cos\alpha_0}\sqrt{M}(1-\kappa)\,\mathrm{cn}\left(\sqrt{M}\;\hat{s}\;|\,1-\kappa\right)\mathrm{sn}\left(\sqrt{M}\;\hat{s}\;|\,1-\kappa\right)$$

where $\mathrm{cn}(u\,|\,m)$ and $\mathrm{sn}(u\,|\,m)$ are additional Jacobi elliptic functions. These solution are valid for positive values of striking yaw α_0. Solutions for negative values of α_0 can be obtained in a similar manner.

Figure 2 shows the typical yawing motion for this case for a representative value of κ. From a small initial striking yaw, the yaw grows rapidly to 90 degrees. Beyond 90 degrees, yaw growth continues but eventually slows before reaching 180 degrees and reverses direction. This oscillating motion continues with the yaw bounded between a particular minimum and maximum yaw that depends on the initial striking yaw and yawing rate. This minimum yaw will be greater than 0 and the maximum yaw will be less than 180 degrees for positive striking yaws. The solution shown in Fig. 2 assumes

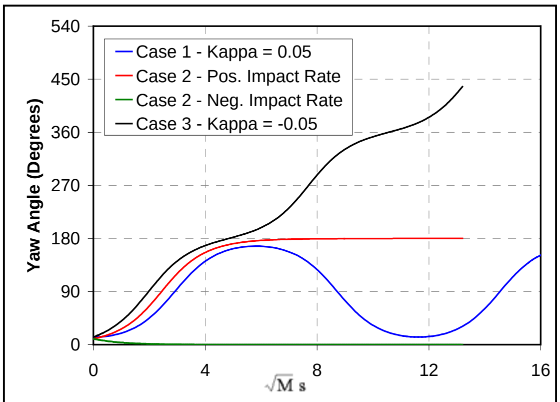

Fig. 2. Typical yawing motion for Case 1, 2 and 3 nonlinear solutions.

zero initial angular rate. However, the yawing behavior for nonzero initial angular rates (for constant values of κ) is also represented by these same curves by appropriate shifting of the solution along the independent variable axis to obtain the proper impact location, based on the correct striking yaw and angular rate.

Case 2 (Neutrally Stable Solutions): $(\kappa = 0)$. Solutions for this case have been previously obtained by Flis. Two valid solutions can be obtained for this case, depending on the initial conditions. For the initial conditions $\alpha_0' = \pm\sqrt{M}\sin\alpha_0$

$$\tan(\alpha/2) = \tan(\alpha_0/2)\exp\left(\pm\sqrt{M}(s - s_0)\right) \tag{11}$$

Figure 2 also shows the typical yawing motion for this case for the same initial striking yaw for positive and negative initial yawing rates. As can be seen for this case, the yaw increases to 180 degrees (bullet flying base first) or decreases to zero. Note that the asymptotic solutions for both sets of initial conditions for Case 2 are neutrally stable solutions. That is, any perturbation to solution will result in the solution diverging from the asymptotic value resulting in a yawing motion resembling Case 1 or Case 3. This can be confirmed by an examination of the governing equation (Eq. 2). Any perturbation in the yaw angle about $\alpha = 0$ or $\alpha = \pi$ will result in a fluid dynamic moment that will tend to increase the yaw angle rather than restore the yaw angle to the asymptotic value. Because these solutions are neutrally stable, it is unlikely that either Case 2 solution will be observed in practice.

Case 3 (Tumbling Solutions): $(\kappa < 0)$. The solution for the third case is cast in terms of another Jacobi elliptic function $\mathrm{cn}(u\,|\,m)$. For positive striking angular rate, the yaw angle will continuously increase and the solution can be written as follows:

$$\alpha = \pi 2n + \sin^{-1}\left[\mathrm{cn}\left(\sqrt{M(1-\kappa)}(s - s_0 + \hat{s})\,\middle|\,\frac{1}{1-\kappa}\right)\right] \tag{12}$$

over the interval $2K \le s - s_0 + \hat{s} - n4K \le 4K$ where K is the period of the elliptic function and n is an integer so that $0 \le s - s_0 + \hat{s} - n4K \le 4K$ and

$$\alpha = \pi(2n-1) - \sin^{-1}\left[\mathrm{cn}\left(\sqrt{M(1-\kappa)}(s - s_0 + \hat{s})\,\middle|\,\frac{1}{1-\kappa}\right)\right] \tag{13}$$

over the interval $0 \le s - s_0 + \hat{s} - n4K \le 2K$. Solutions for negative striking angular rate are easily obtained and have a similar form. $\hat{s}$ is determined from the initial conditions (assuming the striking yaw is $-\pi/2 \le \alpha_0 \le \pi/2$) so that the following two conditions are satisfied so that $0 \le \hat{s} \le 4K$. $\sin\alpha_0 = \mathrm{cn}\left(\sqrt{M(1-\kappa)}\,\hat{s} \mid \frac{1}{1-\kappa}\right)$ and $\alpha_0' = \frac{-1}{\cos\alpha_0}\sqrt{M(1-\kappa)}\,\mathrm{dn}\left(\sqrt{M(1-\kappa)}\,\hat{s} \mid \frac{1}{1-\kappa}\right)\mathrm{sn}\left(\sqrt{M(1-\kappa)}\,\hat{s} \mid \frac{1}{1-\kappa}\right)$.

For initial striking yaw angles between $-\pi/2 \le \alpha_0 \le \pi/2$ and positive striking angular rate, the solution in Eq. 12 describes the initial yaw motion between the striking yaw and $\pi/2$ with $n = 0$. The solution in Eq. 13 describes the subsequent yawing motion for yaw angles between $\pi/2$ and $3\pi/2$ with $n = 1$. As the yaw continues to increase, the description of the yaw alternates between Eq. 12 and 13 with the integer n being incremented by one over the previous cycle of motion.

Figure 2 also shows the typical yawing motion for Case 3 for a representative value of κ. Like the other solutions, the yaw grows rapidly to 90 degrees. However, unlike the Case 1 and 2 solutions, the yaw continues to grow beyond 180 degrees. Beyond 180 degrees, the motion essentially repeats itself as the bullet continues to tumble. The solution shown here assumes a positive initial rate that drives the motion to increasing positive yaw angles. Solutions for negative initial angular rates are obviously possible and drive the yaw to increasing negative yaw angles.

The solutions show, for a fixed striking yaw α_0, the type of motion that results depends on the striking yawing rate. If the striking yawing rate is low enough (Case 1), the motion will be oscillatory. However, if the striking yawing rate becomes large (Case 3), the projectile will tumble because the initial yawing rate is enough to overcome the applied fluid dynamic moment throughout the penetration event. Case 2 represents a limiting case between the two regimes.

As mentioned previously, Roecker used a numerically derived nonlinear solution to successfully fit his experimental data. Flis later obtained essentially the same solution analytically (presented as Case 2 here). The nonlinear exponential yaw growth model, based on Roecker's numerical solution and Flis's analytical solution is shown in Eq. 14.

$$\tan(\alpha/2) = \tan(\alpha_{ref}/2)\exp\left(\sqrt{M}\,s\right) \tag{14}$$

α_{ref} is an arbitrarily selected constant reference angle. The nonlinear exponential yaw growth model reduces to the linear exponential yaw growth model for small angles.

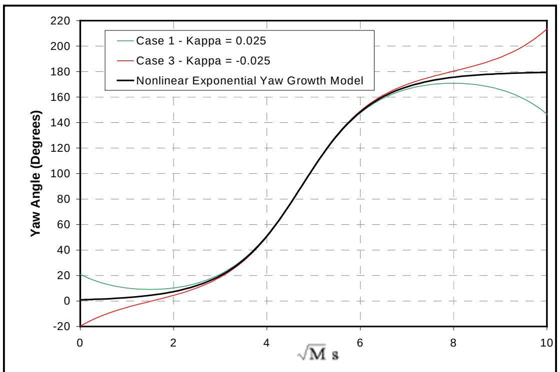

Fig. 3. Comparison of shifted Case 1 and 3 solutions nonlinear exponential yaw growth model.

By shifting the solutions along the independent axis (Fig. 3) so that the solutions coalesce at $\alpha = \pi/2$, it becomes apparent that the nonlinear yaw growth model represents the yaw growth over a significant portion of the penetration event. The angular rates at $\alpha = \pi/2$ for each solution are similar but not equal for small values of κ by virtue of Eq. 8. Like the linear solution, the nonlinear yaw growth model (Eq. 14) only represents the yaw growth after a sufficient depth of penetration and there is a transitional region where the yaw growth is more properly represented by the complete solutions (Eqs. 9 and 10 or 12 and 13) unless, of course, the boundary conditions produce the Case 2 solution.

CONCLUSION

A complete set of analytical solutions for the linear and nonlinear yaw growth of a projectile impacting and traversing dense media is presented. The solutions are used to expose important attributes of the yawing behavior of projectiles in dense media. The results show that for a sufficient depth of penetration, the yaw growth can be characterized by Roecker's linear and nonlinear yaw growth models, but there is a transitional region early in the penetration event, where the more complete solution is required to characterize the yaw growth. The solutions also show that the nonlinear yawing motion is characterized by oscillating motion at yaw angles of less than 180 degrees or by an end-over-end tumbling motion, depending on the striking yaw and yawing rate.

REFERENCES

[1] E.T. Roecker and A.J. Ricchiazzi, "Stability of Penetrators in Dense Fluids," *Journal of Engineering Science*, Vol. 16, pp. 917-920, 1978.

[2] W.J. Flis, "A Note on the Roecker-Ricchiazzi Model of Penetrator Trajectory Instability," Proceedings of the 22nd International Symposium on Ballistics, Vol. 2, DEStech Publications, Inc., Lancaster, PA, pp. 1287-1294, 2005.